Temperature-dependent exchange stiffness and domain wall width in Co

R. Moreno,[1] R. F. L. Evans,[2] S. Khmelevskyi,[3] M. C. Muñoz,[1] R. W. Chantrell,[2] and O. Chubykalo-Fesenko[1]

[1]*Instituto de Ciencia de Materiales de Madrid, CSIC, Cantoblanco, 28049 Madrid, Spain*
[2]*Department of Physics, University of York, Heslington, York, YO10 5DD, United Kingdom*
[3]*Center for Computational Materials Science, Vienna University of Technology, A-1040, Vienna, Austria*

The micromagnetic exchange stiffness is a critical parameter in numerical modeling of magnetization dynamics and reversal processes, yet the current literature reports a wide range of values even for such simple and widely used material as cobalt. Using the *ab initio* estimated Heisenberg parameters we calculate the low temperature micromagnetic exchange stiffness for hexagonal-close-packed (hcp) and face-centered-cubic cobalt. For hcp Co they are slightly different in the directions parallel and perpendicular to the c axis. We establish the exchange stiffness scaling relation with magnetization $A(m) \sim m^{1.8}$ valid for a wide range of temperatures. For hcp Co we find an anisotropic domain wall width in the range 24–29 nm which increases with temperature. The results form a critical input for large-scale temperature-dependent micromagnetics simulations and demonstrate the importance of correct parametrization for accurate simulation of magnetization dynamics.

I. INTRODUCTION

Many recent applications with appealing technological perspectives are based on the magnetization dynamics at high temperatures. These include magnetization dynamics under thermal gradients (spin-Seebeck effect) [1], ultrafast laser-induced magnetization dynamics [2], or heat-assisted magnetic recording [3]. The usual way to model magnetization dynamics in nanostructures is numerical micromagnetics for which publicly released codes are widely used. Strictly speaking the standard micromagnetics is a zero or low temperature approximation although the temperature-dependent macroscopic parameters can be used far from the Curie temperature T_C. Recently high-temperature micromagnetics based on the use of the Landau-Lifshitz-Bloch equation [4–6] has been developed, removing the constraint of the fixed magnetization magnitude. For correct modeling the zero temperature micromagnetic parameters and their temperature dependence are required.

The temperature dependence of micromagnetic parameters can be in principle measured experimentally. This is straightforward for the saturation magnetization, but more challenging for the correct macroscopic anisotropy and the exchange stiffness constants. A limitation of the experimental approach is that extrinsic (dependence on defects) and intrinsic (the proper temperature dependence) effects cannot be distinguished, nor can different contributions to the macroscopic parameters be determined, for example, coming from interfacial as compared to the bulk anisotropy. In this respect modeling provides a unique method to assess the correct values of these parameters.

For the correct use of micromagnetics the exchange stiffness A is one of the most important parameters since it defines the exchange correlation length measuring the Bloch domain wall thickness $\delta_{DW} = \pi \sqrt{(A/K)}$, where K is the macroscopic anisotropy constant. However the literature reveals a large discrepancy in the value of this parameter for cobalt.

Hexagonal-close-packed (hcp) cobalt is the classic high anisotropy magnetic material widely used due to its high Curie temperature and large magnetocrystalline anisotropy in the bulk. Additives such as Pt and Sm enable hcp Co-based magnets to be used in current magnetic recording media and permanent magnets, respectively. Yet, Co is not so simple.

According to the measurements, hcp Co undergoes transition to the face-centered-cubic (fcc) phase [7] at temperatures around $T = 695$ K and at around the same temperature the magnetization easy axis turns perpendicular to the c-axis direction [8].

Micromagnetic simulations frequently assume values of the exchange stiffness in Co in two different ranges: $(1.3–1.5) \times 10^{-11}$ J/m (e.g., [9,10]) or $(2.2–3.3) \times 10^{-11}$ J/m (e.g., [11–13]). The experimental measurements on the exchange stiffness using Brillouin light scattering report values between 2.5×10^{-11} [14] and 3.6×10^{-11} J/m [15]. At the same time old and forgotten neutron scattering data show higher values of 4.2×10^{-11} J/m [16]. The differences are normally attributed to nonhomogeneous pinned spin structures due to grain boundaries in nonperfect samples [15].

Typically the Bloch domain wall width in hcp Co is assumed to be between 10 and 15 nm, following classical books in magnetism (e.g., Refs. [17,18]). We note here that the use of different exchange stiffness values may completely alter the result of a micromagnetic simulation since it defines the occurrence of different reversal modes, associated with different coercivities, as well as it may change the type of the reversal mode, for example from transverse to the vortexlike domain wall in hcp Co nanowires [19].

It is well known that both the anisotropy and the exchange stiffness in magnetic materials decrease with temperature. Since typically anisotropy decreases faster than the exchange stiffness, the domain wall width increases with temperature, which is widely observed experimentally (see, for example, Ref. [20]). The correct temperature dependence of the exchange stiffness is important for applications since it may define the transition from incoherent to coherent reversal modes as well as change the domain wall velocity. Also, the change in the domain wall width with temperature has been determined as the key factor in its motion under thermal gradients [21] as well as for the ultrafast magnetization dynamics response [22]. Thus accurately determining the rate of change of the domain wall width with temperature is very important from both fundamental and applied points of view.

In the present article starting with parametrizations of the Heisenberg Hamiltonian with *ab initio* electronic structure

calculations, we evaluate the exchange stiffness parameter and the domain wall width as a function of temperature. We determine the domain wall width at low temperatures as large as 24–29 nm, depending on the Heisenberg model parametrization. This value is larger than frequently assumed, and it increases with temperature. We also determine the scaling relation with magnetization of both the exchange stiffness parameter and the domain wall width.

II. MODELING RESULTS

A. The Heisenberg exchange parametrization

To evaluate the domain wall width and the exchange stiffness in Co, we use a hierarchical multiscale approach, proposed for FePt by Kazantseva *et al.* [5,23]. We define the atomic exchange parameters for Co for the Heisenberg spin Hamiltonian

$$\mathcal{H} = -\frac{1}{2} \sum_{i \neq j} J_{ij} \mathbf{S}_i \cdot \mathbf{S}_j - \sum_i k_u S_z^2, \tag{1}$$

where $\mathbf{S}_i$ are classical unit vectors describing the magnetic moment directions on site i, J_{ij} is the interatomic exchange interaction, and k_u is the local uniaxial anisotropy constant per atom.

The long-range pairwise exchange parameters can be evaluated on the basis of *ab initio* methods by mapping the electronic structure calculation onto the Heisenberg model. The first set of these parameters for hcp Co at $T = 0$ K was evaluated by Turek *et al.* [24] and for fcc Co by Pajda *et al.* [25] with experimental lattice parameters. Very recently a new set of data has been published by Kvashnin *et al.* [26]. Since the calculated exchange parameters in these works are different, we have performed our own calculations of the Heisenberg exchange parameters (see Table I).

Our first-principles calculation is based on the local spin-density approximation and bulk Korringa-Kohn-Rostokker (KKR) method in the atomic sphere approximation (ASA) [27,28]. The partial waves in the KKR-ASA calcula-

TABLE I. Calculated exchange parameters for hcp and fcc cobalt up to the first six shells. R_{0j} is the shell position in units of lattice constant and N_s is the number of equivalent sites in the shell.

	Co (hcp)			Co (fcc)	
R_{0j}	N_s	J_{0j} (mRy)	R_{0j}	N_s	J_{0j} (mRy)
(100)	6	1.77	$(\frac{1}{2}\frac{1}{2}0)$	12	1.87
$(\frac{1}{2}\frac{1}{2\sqrt{3}}\sqrt{\frac{2}{3}})$	6	2.08			
$(1\frac{-1}{\sqrt{3}}\sqrt{\frac{2}{3}})$	6	0.28	(100)	6	0.16
$(00\sqrt{\frac{8}{3}})$	2	0.49	$(1\frac{1}{2}\frac{1}{2})$	24	0.21
$(0\sqrt{30})$	6	0.21	(110)	12	−0.23
$(1\frac{2}{\sqrt{3}}\sqrt{\frac{2}{3}})$	12	0.18			
$(10\sqrt{\frac{8}{3}})$	12	−0.06	$(\frac{3}{2}\frac{1}{2}0)$	24	0.06
(200)	6	−0.15	(111)	8	0.09

TABLE II. Results for different Co hcp parametrizations.

	Turek *et al.* [24]	Kvashnin *et al.* [26]	This work
Exchange stiffness			
Plane xy (10^{-11} J/m)	4.38	2.95	3.33
c axis (10^{-11} J/m)	4.73	3.02	3.62
Domain wall width		$T = 0$ K	
Plane xy (nm)	28.49	23.42	24.88
c axis (nm)	29.60	23.70	25.96
CSDM			
ε	0.186	0.208	0.207
	$A \sim m^{1.81}$	$A \sim m^{1.79}$	$A \sim m^{1.79}$
T_C (K)	1480	1100	1250

tions have been expanded up to the orbital $l_{\max} = 3$ (*spdf* basis) inside the atomic spheres, for all nonequivalent atomic sites. The exchange parameters have been calculated using the magnetic force theorem [29]. The exchange constants were estimated in ferromagnetic ground state at $T = 0$ K, which give a reasonable estimation also at nonzero temperatures for both fcc and hcp Co. Our method of the exchange constants calculation is essentially the same as that of Pajda *et al.* [25], however, we used a more extended basis for partial wave expansion ($l_{\max} = 3$) than Pajda *et al.* who used $l_{\max} = 2$. Because of that our exchange constants are closer to Kvashnin *et al.* [26], who used a full potential methodology. Previously, the application of our approach has allowed a successful description of magnetism in various transition metal systems [30,31].

The exchange parameters show dominant ferromagnetic interactions up to the third nearest neighbors and the typical RKKY oscillating asymptote. In what follows we include the exchange interactions up to six nearest neighbors. To evaluate temperature-dependent properties we use classical Langevin dynamics simulations based on the integration of a set of stochastic Landau-Lifshitz-Gilbert (LLG) equations [32] with internal fields defined by the Hamiltonian (1). The resulting Curie temperatures are summarized in Tables II (hcp Co) and III (fcc Co) for the different sets of parameters. The $T_C = 1480$ K value, which we calculate here by the Langevin dynamics approach with the parameters of Turek *et al.* is close to the most frequently cited experimental value for Co $T_C = 1385$ K (e.g., the book [18] measured in [33,34]). Because of that agreement, this parametrization gives a suitable for magnetization dynamics modeling curve $M(T)$ and we therefore use values from Turek *et al.* [24] in the dynamical simulation of the domain wall width. The Curie temperatures for both hcp ($T_C = 1250$ K) and fcc ($T_C = 1300$ K) phases calculated with our parameters are also close to the experimental one

TABLE III. Results for different Co fcc parametrizations.

	Pajda *et al.* [25]	This work
Exchange stiffness (10^{-11} J/m)	4.41	3.62
CSDM	$\varepsilon \sim 0.177$	$\varepsilon \sim 0.180$
	$A \sim m^{1.82}$	$A \sim m^{1.82}$
T_C (K)	1550	1300

(see Table I) although they are below it. At the same time the calculations with parameters by Kvashnin *et al.* [26]) give a smaller Curie temperature $T_C = 1100$ K but in agreement with the value of 1131 K cited in the book by Cullity [35].

We note that our estimations of T_C do not include the effects of longitudinal spin fluctuations at high temperatures and renormalization of the exchange constants due to the spin disorder in a paramagnetic state [28]. Thus the obtained T_C values cannot be considered as a test of the exchange constants quality which are calculated from the low temperature ferromagnetic reference state. Besides, namely the exchange constants calculated in the ferromagnetic ground state should be used at the temperatures much lower than experimental magnetic ordering temperature. Note that within the disordered local moment approach the temperature dependence of the Heisenberg exchange coupling constants for hcp Co has been found to be very weak [36] in the considered here range of temperatures.

Finally, experimentally hcp Co has been reported to undergo a transition to the fcc structure [7] at temperatures around $T = 695$ K. Since the dependence of the Curie temperature on the structure is found here to be small, this transition could be disregarded in relation to the exchange stiffness evaluation.

B. Exchange stiffness: Analytical approach

The calculated *ab initio* Heisenberg exchange parameters allow the evaluation of the exchange stiffness at zero temperature via the formula

$$A^\nu(0) = [1/(4V_{at})] \sum_j J_{0j}^\nu \left(r_0^\nu - r_j^\nu\right)^2, \qquad (2)$$

which can be obtained assuming the continuous long-wavelength function for the spin distribution in the Heisenberg Hamiltonian. This formula is a generalization of the one found in the classical books (see, for example, [37]). Here V_{at} is the atomic volume (we assume the experimental value $V_{at} = 1.1 \times 10^{-29}$ m^3), r_j are the atomic positions from the origin, and $\nu = x, y, z$ stands for Cartesian coordinates. Assuming that the c axis of hcp Co coincides with the z axis, we obtain slightly different exchange stiffness parameters, parallel and perpendicular to it, summarized for different sets of parameters in Table II.

For the fcc Co the obtained exchange stiffness value is isotropic and similar to the hcp value. The obtained values are similar to the upper bound or larger than typically used in micromagnetic simulations, frequently by a factor of 2. They are also close to the upper bound measured by the Brillouin scattering [15].

To determine the theoretical exchange stiffness scaling with magnetization (i.e., temperature), we employ the classical spectral density method (CSDM) for spinwaves [38,39], previously shown to have a good agreement with the Langevin dynamics simulations in simple cubic lattice materials and FePt [39,40]. The method is based on the use of Green's functions in reciprocal space which first leads to an infinite set of coupled equations for thermally averaged moments of all orders. The spectral density is assumed to be a delta function. The following decoupling scheme which leaves the equations for the first two moments only (found to be sufficient for the

exchange interactions [38,39]) is then assumed:

$$\langle S_{\mathbf{k}}^z S_{-\mathbf{k}}^z \rangle \cong \langle S_{\mathbf{k}}^z \rangle \langle S_{-\mathbf{k}}^z \rangle - \tfrac{1}{2}(1 - m^2)\langle S_{\mathbf{k}}^+ S_{-\mathbf{k}}^- \rangle, \qquad (3)$$

where m is the average magnetization, $S_{\mathbf{k}}^\pm$ is the Fourier transform of $S_i^\pm = S_i^x \pm S_i^y$ variables, and $S_{\mathbf{k}}^z$ of S_i^z variable. The Fourier transform of the exchange parameters is defined in terms of the variable

$$\gamma_{\mathbf{q}} = \frac{J(\mathbf{q})}{J(0)} = \sum_j \frac{J_{0j}}{J(0)} e^{-i\mathbf{q}\cdot(\mathbf{r}_0 - \mathbf{r}_j)}, \qquad (4)$$

where $J(0)$ is the is the zero wave-vector component $J(0) = z_1 J_{01} + z_2 J_{02} + \cdots$, z_{0j} is the number of neighbors with the same J_{0j} interaction, and $\vec{r}_0$ and $\vec{r}_j$ are position vectors of the atoms 0 and j, respectively. The decoupled equations give the following dispersion relation [39]:

$$\omega_{\mathbf{q}} = J_0 m Q(m)(1 - \gamma_{\mathbf{q}}), \qquad (5)$$

where at low temperatures the function $Q(m)$ scales with magnetization m as $Q(m) \propto m^{-\varepsilon}$ and the scaling parameter ε is defined by the ratio of the sums $\varepsilon = G/W$:

$$W = \sum_{\mathbf{q}} \frac{1}{1 - \gamma_{\mathbf{q}}}, \quad G = \sum_{\mathbf{q}} \frac{\gamma_{\mathbf{q}}}{1 - \gamma_{\mathbf{q}}}. \qquad (6)$$

These sums were numerically evaluated over the first Brillouin zone giving $\varepsilon \approx 0.19$ for parameters of Turek *et al.* [24] and $\varepsilon \approx 0.21$ for the other two sets. The spinwave dispersion relation (5) is directly related to the exchange stiffness parameter leading to the scaling relation $A(T) = A(0)m^{2-\varepsilon} \propto m^{1.8}$ for all cases (see Tables II and III for more precise values). The difference with the mean-field exponent $\varepsilon = 2$ comes from spin-spin correlations [39]. This result is compared in Fig. 3 with direct estimations of the exchange stiffness parameter via the temperature-dependent domain wall width simulations (see below), showing good agreement up to very high temperatures. To reconcile different approaches we have presented normalized values $A(T)/A(0)$ as a function of normalized temperature T/T_C. A very similar scaling exponent ensures that for normalized values the results are almost the same for all models.

C. Modeling of the temperature-dependent domain wall width

The domain wall width depends on the anisotropy value. The *ab initio* estimation of this value is difficult and not very reliable. To be more specific, we simply use an experimental realistic value for hcp Co $k_u = 5.83 \times 10^{-24}$ J/atom, corresponding to the macroscopic constant $K = 0.53 \times 10^6$ J/m^3 [41]. Note that a constant atomic anisotropy value gives a temperature-dependent macroscopic anisotropy. There may be an additional temperature dependence of the on-site anisotropy which is difficult to estimate. Specifically, the intrinsic change of anisotropy happens via the temperature-induced transformation from hcp to fcc structure. However, we note that a different anisotropy value changes the domain wall width but is not important for the determination of the temperature dependence of the exchange stiffness parameter.

The evaluated hcp exchange stiffness parameter and the anisotropy value $k_u = 5.83 \times 10^{-24}$ J/atom via the formula $\delta_{DW} = \pi\sqrt{A/K}$ gives the zero-temperature domain wall
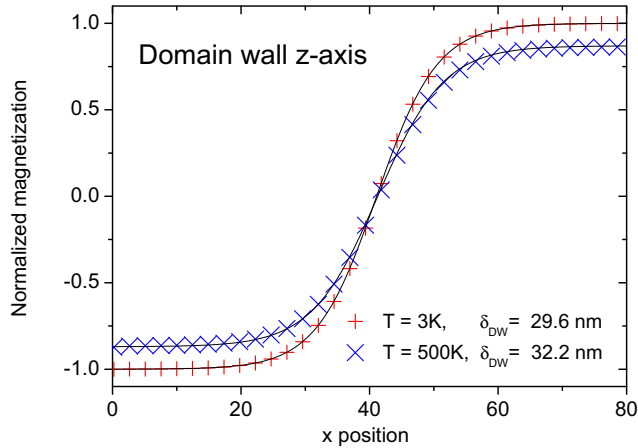
FIG. 1. Simulated domain wall profiles (crosses) for temperatures $T = 3$ K and $T = 500$ K, using the exchange values of Turek *et al.* [24] showing a reduction in the equilibrium magnetization at elevated temperature and an increase in the domain wall width from 29.6 to 32.3 nm. The lines shows the fitting to the domain wall profile, Eq. (7).
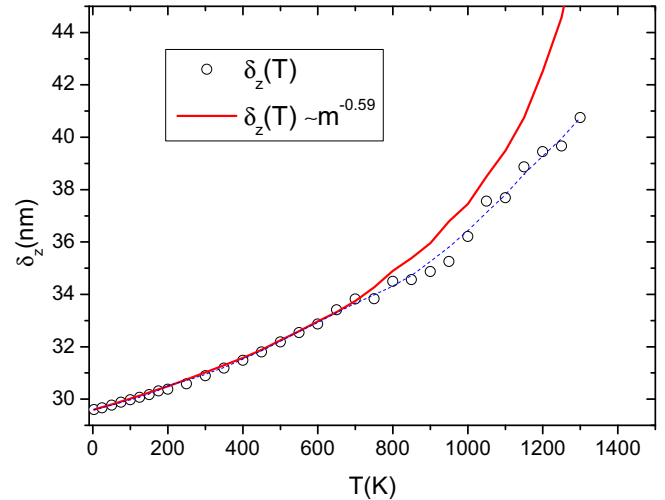

FIG. 2. Temperature dependence of the domain wall width (normalized to $T = 0$ K value). The symbols indicate the data extracted from direct simulations, while the solid line line shows a low temperature scaling law with magnetization $\delta_{DW} \sim m^{-0.59}$. The dashed line is the guideline corresponding to the smoothed data.

widths summarized in Table II . The widths are slightly different parallel and perpendicular to the *c*-axis direction. For values from Turek *et al.* [24] they are as large as 29 nm, while the two other sets of parameters give smaller values around 24–25 nm. In any case these values are significantly larger than the range 10–15 nm cited in classical books [17,18].

The domain wall width at any temperature can be modeled directly by Langevin dynamics simulations using the parametrized Heisenberg Hamiltonian (1). For this purpose we have used two codes for atomistic simulations: our homemade one as well as the publicly available VAMPIRE code [32,42]. We used a system size of up to 80 nm in length and with a cross-sectional area of 250 nm^2 in order to fully contain the domain wall. The domain wall is constrained in the system by applying antiperiodic boundary conditions. The resulting domain wall profile for two temperatures is presented in Fig. 1, based on the parameters of Turek *et al.* [24]. The results clearly show an increase in the domain wall width with temperature.

To determine the domain wall width from the simulations, we fit the magnetization profile to

$$m_z(x) = m_e \tanh[\pi(x - x_0)/\delta_{DW}], \tag{7}$$

where m_e is the equilibrium magnetization. The results are in excellent agreement with analytical estimations presented in Table II. For example, using the parameters of Turek *et al.* [24] we obtain for low temperatures $\delta_{DW}^x = 28.50$ nm, $\delta_{DW}^z = 29.59$ nm with our program and $\delta_{DW}^x = 28.50$ nm, $\delta_{DW}^z = 29.57$ nm with the VAMPIRE code in a very good agreement with our direct estimation of $\delta_{DW}^x = 28.49$ nm and $\delta_{DW}^z = 29.60$ nm.

Next, the domain wall profile was evaluated at all temperatures up to the Curie temperature, see Fig. 2, showing a clear increase of the domain wall width with temperature. The logarithm of the low-temperature part of the domain wall width can be fitted to a power law as a function of magnetization. This way we obtained low-temperature scaling behavior $\delta_{DW} \sim m^{-0.59}$ in both *x* and *z* directions. The

comparison of this scaling law with the domain wall width extracted from the direct simulations, shows that it correctly describes the behavior up to temperatures around 800 K, see Fig. 2. We stress again that we have not taken into account here the transition to fcc structure which would result in strong anisotropy decrease and further increase the domain wall width with temperature.

D. Modeling of the temperature-dependent exchange stiffness

The simulated temperature dependence of the domain wall width allows the temperature dependence of the exchange stiffness parameter A to be calculated via the formula $\delta_{DW} = \pi\sqrt{A/K}$. For this purpose we first evaluate the temperature dependence of the macroscopic anisotropy K using the constrained Monte Carlo method [43], implemented in the VAMPIRE code. The evaluation shows that the macroscopic anisotropy closely follows the Callen-Callen law $K(m) \sim m^3$ practically up to 1200 K. Using the temperature-dependent values of the anisotropy and the domain wall width resulting from our simulations we calculate the exchange stiffness for the whole temperature range, as shown in Fig. 3. The simulated data are compared with the CSDM prediction of the scaling behavior $A(T) \sim m^{1.81}$ showing a good agreement up to very high temperatures.

Finally, we recall that the classical Heisenberg model leads to a temperature-dependent magnetization $m(T)$ described by the Langevin function. This functional form typically is not in agreement with the experimentally measured one, particularly for hcp Co [44], which is known to be better described by the Brillouin function with $S = 1/2$ [35]. Thus the low and high temperature experimental and our asymptotes for $m(T)$ are significantly different. For example, at low temperatures the Langevin function gives a linear dependence on temperature, while the Brillouin function gives the well-known $1 - \text{const}(T/T_C)^{3/2}$ Bloch law. Note that in terms of
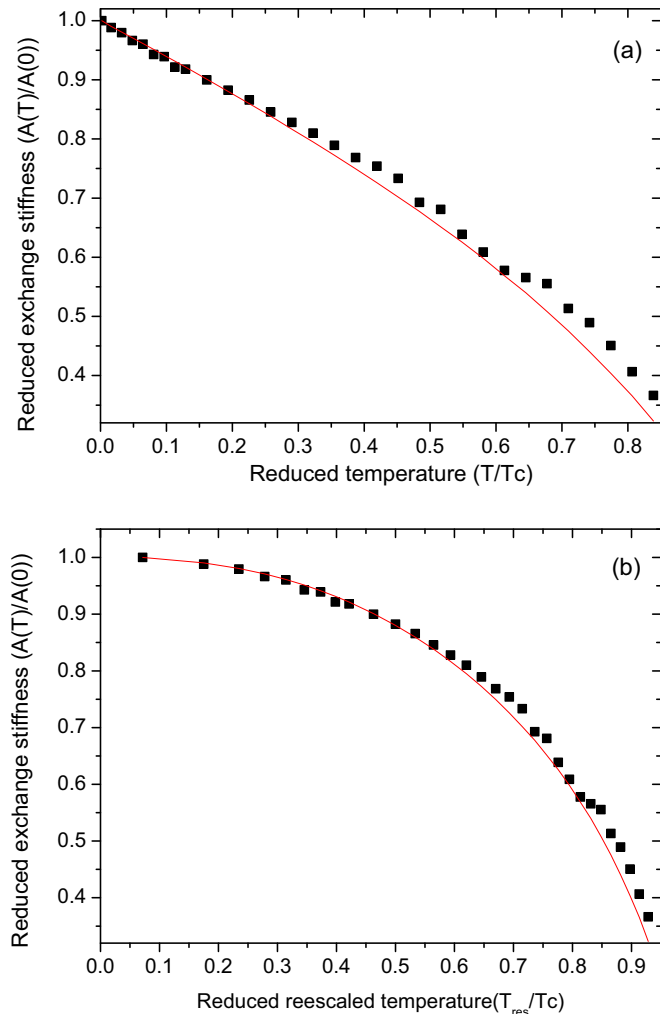
FIG. 3. Temperature dependence of the exchange stiffness parameter from atomistic simulations and theory. The symbols indicate the data extracted from direct evaluation of the domain wall profile. The line plots the scaling relation $A(T) = A(0)m^{1.8}$. (a) The data obtained via the direct estimation in the classical Heisenberg model while (b) represents the rescaled data according to Eq. (8).

the magnetization (and not temperature) the classical and quantum cases give similar behavior [40]. To overcome the problem of the incorrect temperature dependence of the magnetization in the simulation and to make our results more useful for comparison with experiments, we assume that the experimentally measured magnetization obeys the Curie-Bloch relation $m(T) = [1 - (T/T_C)^\alpha]^\beta$ with $\beta = 0.34$ and $\alpha = 2.369$ for Co [45]. We then apply temperature rescaling as suggested in Ref. [45] with the function

$$\frac{T}{T_C} = \left(\frac{T_{res}}{T_C}\right)^\alpha,$$ (8)

where T_{res} is a new (experimental) temperature. The resulting temperature dependence of the stiffness parameter is shown in Fig. 3(b) taking into account the correct temperature dependence of the magnetization fluctuations.

III. CONCLUSIONS

In conclusion, using a multiscale approach we have estimated the temperature-dependent domain wall width and the exchange stiffness parameter in Co. We have used two parametrizations of the Heisenberg Hamiltonian available in the literature as well as our own.

The low temperature values for the exchange stiffness parameter appear to be frequently larger than the widely used ones and more consistent with upper estimation by the Brillouin scattering method [15] and even with old neutron measurements [16]. The values appear to be very similar for fcc and hcp Co. The domain wall width for hcp Co at low temperatures was found to be in the interval 24–29 nm. By means of the theoretical CSDM and direct Langevin dynamics simulations we have found the magnetization scaling exponents for both domain wall width ($\delta_{DW} \sim m^{-0.6}$, hcp Co) and the exchange stiffness ($A \sim m^{1.8}$) parameters. Note that in the fitting of numerical data, the differences between the approximate scaling exponents 0.6 for the domain wall width and 1.8 for the exchange stiffness and the ones with more digits obtained from the theory are not distinguishable. Consequently, we may say that these exponents are almost the same for different parametrizations. The exchange stiffness scaling exponent is also the same for fcc and hcp Co. The agreement between direct estimations from the domain wall width and the classical spectral density method gives us confidence in our results.

Our findings are important for both zero and high-temperature micromagnetics, as they may change the boundaries between the occurrence of different reversal modes. They could lead to markedly different results for simulations of the spin-Seebeck effect or high temperature domain wall dynamics. We stress that the multiscale approach is essentially parameter free since all input parameters to the atomistic spin model are determined from *ab initio* calculations. We suggest that, although our estimates of exchange stiffness are at the upper end of the spectrum of experimental values, our model calculations provide an important benchmark for the fundamental magnetic properties of Co.

[1] K. Uchida, S. Takahashi, K. Harii, J. Ieda, W. Koshibae, K. Ando, S. Maekawa, and E. Saitoh, Nature (London) **455**, 778 (2008).

[2] T. A. Ostler, J. Barker, R. F. L. Evans, R. W. Chantrell, U. Atxitia, O. Chubykalo-Fesenko, S. El Moussaoui, L. Le Guyader, E. Mengotti, L. J. Heyderman, F. Nolting, A. Tsukamoto, A. Itoh,

D. Afanasiev, B. A. Ivanov, A. M. Kalashnikova, K. Vahaplar, J. Mentink, A. Kirilyuk, Th. Rasing, and A. V. Kimel, Nat. Commun. **3**, 666 (2012).

[3] M. H. Kryder, E. C. Gage, T. W. McDaniel, W. A. Challener, R. E. Rottmayer, G. Ju, Y.-T. Hsia, and M. F. Erden, Proc. IEEE **96**, 1810 (2008).

[4] D. A. Garanin, Phys. Rev. B **55**, 3050 (1997).

[5] N. Kazantseva, D. Hinzke, U. Nowak, R. W. Chantrell, U. Atxitia, and O. Chubykalo-Fesenko, Phys. Rev. B **77**, 184428 (2008).

[6] R. F. L. Evans, D. Hinzke, U. Atxitia, U. Nowak, R. W. Chantrell, and O. Chubykalo-Fesenko, Phys. Rev. B **85**, 014433 (2012).

[7] P. Toledano, G. Krexner, M. Prem, H.-P. Weber, and V. P. Dmitriev, Phys. Rev. B **64**, 144104 (2001).

[8] W. Sucksmith and J. E. Thompson, Proc. Royal Soc. A **225**, 1162 (1954).

[9] H. F. Ding, W. Wulfhekel, and J. Kirschner, Europhys. Lett. **57**, 100 (2002).

[10] S. Pathak and M. Sharma, Adv. Mat. Lett. **3**(6), 526 (2012).

[11] H. F. Ding, A. K. Schmid, D. Li, K. Yu. Guslienko, and S. D. Bader, Phys. Rev. Lett. **94**, 157202 (2005).

[12] M. Grujicic and B. Pesic, J. Magn. Magn. Mater. **285**, 303 (2005).

[13] K.-J. Lee, A. Deac, O. Redon, J.-P. Noziéres, and B. Dieny, Nat. Mater. **3**, 877 (2004).

[14] S. P. Vernon, S. M. Lindsay, and M. B. Stearns, Phys. Rev. B **29**, 4439 (1984).

[15] M. Grimsditch, E. E. Fullerton, and R. L. Stamps, Phys. Rev. B **56**, 2617 (1997).

[16] G. Shirane, V. J. Minkiewicz, and R. Nathans, J. Appl. Phys. **39**, 383 (1968).

[17] E. Kneller, *Ferromagnetism* (Springer, Berlin, 1962).

[18] R. C. O'Handley, *Modern Magnetic Materials: Principles and Applications*, 1st ed. (Wiley-Interscience, New York, 1999).

[19] Yu. P. Ivanov. M. Vazquez, and O. Chubykalo-Fesenko, J. Phys. D **46**, 485001 (2013).

[20] G. Vértesy and I. Tomáš, J. Appl. Phys. **93**, 4040 (2003).

[21] J. Chico, C. Etz, L. Bergqvist, O. Eriksson, J. Fransson, A. Delin, and A. Bergman, Phys. Rev. B **90**, 014434 (2014).

[22] M. B. Pfau, S. Schaffert, L. Müller, C. Gutt, A. Al-Shemmary, F. Büttner, R. Delaunay, S. Düsterer, S. Flewett, R. Frömter, J. Geilhufe, E. Guehr, C. M. Günther, R. Hawaldar, M. Hille, N. Jaouen, A. Kobs, K. Li, J. Mohanty, H. Redlin, W. F. Schlotter, D. Stickler, R. Treusch, B. Vodungbo, M. Klaui, H. P. Oepen, J. Lüning, G. Grübel, and S. Eisebitt, Nat. Commun. **3**, 1100 (2008).

[23] D. Hinzke, U. Nowak, R. W. Chantrell, and O. N. Mryasov, Appl. Phys. Lett. **90**, 082507 (2007).

[24] I. Turek, J. Kudrnovský, V. Drchal, P. Bruno, and S. Blügel, Phys. Stat. Sol. (b) **236**, 318 (2003).

[25] M. Pajda, J. Kudrnovsky, I. Turek, V. Drchal, and P. Bruno, Phys. Rev. B **64**, 174402 (2001).

[26] Y. O. Kvashnin, W. Sun, I. Di Marco, and O. Eriksson, Phys. Rev. B **92**, 134422 (2015).

[27] I. A. Abrikosov and H. L. Skriver, Phys. Rev. B **47**, 16532 (1993).

[28] A. V. Ruban and H. L. Skriver, Comput. Mater. Sci. **15**, 119 (1999).

[29] A. I. Liechtenstein, M. I. Katsnelson, V. P. Antropov, and V. A. Gubanov, J. Magn. Magn. Mater. **67**, 65 (1987).

[30] S. Khmelevskyi and P. Mohn, Appl. Phys. Lett. **93**, 162503 (2008).

[31] S. Khmelevskyi, E. Simon, and L. Szunyogh, Phys. Rev. B **91**, 094432 (2015).

[32] R. F. L. Evans, W. J. Fan, P. Chureemart, T. A. Ostler, M. O. A. Ellis, and R. W. Chantrell, J. Phys.: Condens. Matter **26**, 103202 (2014).

[33] H. P. Myers and W. Sucksmith, Proc. R. Soc. London A **207**, 427 (1951).

[34] J. Crangle, Philos. Mag. **46**, 499 (1955).

[35] B. D. Cullity, *Introduction to Magnetic Materials* (Addison-Wesley, Reading, MA, 1972).

[36] D. Bottcher, A. Ernst, and J. Henk, J. Magn. Magn. Mater. **324**, 610 (2012).

[37] A. Aharoni, *Introduction to The Theory of Ferromagnetism*, International Series of Monographs on Physics Vol. 109, 2nd ed. (Oxford University Press, Oxford, 1996).

[38] L. S. Campana, A. Caramico D'Auria, M. D'Ambrosio, U. Esposito, L. De Cesare, and G. Kamieniarz, Phys. Rev. B **30**, 2769 (1984).

[39] U. Atxitia, D. Hinzke, O. Chubykalo-Fesenko, U. Nowak, H. Kachkachi, O. N. Mryasov, R. F. Evans, and R. W. Chantrell, Phys. Rev. B **82**, 134440 (2010).

[40] R. Bastardis, U. Atxitia, O. Chubykalo-Fesenko, and H. Kachkachi, Phys. Rev. B **86**, 094415 (2012).

[41] D. Jiles, *Introduction to Magnetism and Magnetic Materials* (Chapman and Hall, London, 1991).

[42] VAMPIRE software package v.4 http://vampire.york.ac.uk (2015).

[43] P. Asselin, R. F. L. Evans, J. Barker, R. W. Chantrell, R. Yanes, O. Chubykalo-Fesenko, D. Hinzke, and U. Nowak, Phys. Rev. B **82**, 054415 (2010).

[44] M. D. Kuz'min, Phys. Rev. Lett. **94**, 107204 (2005).

[45] R. F. L. Evans, U. Atxitia, and R. W. Chantrell, Phys. Rev. B **91**, 144425 (2015).